Combined Trajectory Simulation and Optimization for Hybrid Rockets using ASTOS and ESPSS

By Christian SCHMIERER,[1),2)] Mario KOBALD,[1)] Johan STEELANT[3)] and Stefan SCHLECHTRIEM[1),2)]

[1)] *Institute of Space Propulsion, German Aerospace Center (DLR), Lampoldshausen, Germany*

[2)] *Institute of Space Systems (IRS), University of Stuttgart, Germany*

[3)] *European Space Research and Technology Centre (ESTEC), European Space Agency (ESA), Netherlands*

(Received April, 17th, 2017)

The combined simulation of propulsion system performance and trajectory is crucial for the design of a space mission. Therefore the trajectory simulation and optimization software ASTOS is used together with the rocket propulsion simulation tool EcosimPro/ESPSS to simulate and optimize different missions for launcher and spacecraft applications. A special focus is put on hybrid rocket engines. This class of rocket engines is advancing at a high speed and applications in different fields are investigated and developed. High safety, low cost and using "green" propellants makes hybrid rocket engines a viable choice for a propulsion system. A simulation toolset for ASTOS to calculate and optimize hybrid rocket engine performance is developed. A connection to the dedicated propulsion simulation tool ESPSS is implemented to further improve the simulation of hybrid rocket engines in a loop with the trajectory design. The software interface is successfully implemented and first optimization results look very promising.

Key Words: Hybrid Rockets, Trajectory, Simulation, Optimization

Nomenclature

a	:	regression rate coefficient
c^*	:	characteristic velocity
c_F	:	thrust coefficient
G	:	mass flux
h	:	enthalpy
n	:	regression rate exponent
$\dot{r}$	:	regression rate
u	:	velocity
x	:	position
η	:	efficiency
μ	:	dynamic viscosity
ρ	:	density
Subscripts		
c	:	conditions at the flame
e	:	boundary layer edge
f	:	fuel
m	:	mean
ox	:	oxidizer
vap	:	vaporization

1. Introduction

Hybrid rockets have received more and more attention for their safety, low-cost and green propellant combinations in recent years all over the world. At the German Aerospace Center (DLR) at Lampoldshausen and at the University of Stuttgart hybrid rocket engines have been researched and developed since 2006. Advanced fuels like paraffin-based fuels have been analyzed for their performance and applicability.[1)] The student team HyEnD of the University of Stuttgart developed, built and launched a hybrid propulsion sounding rocket using paraffin-based fuels and nitrous oxide as an oxidizer.[2)] For future projects it is vital to have the right design and development tools to conceive hybrid rocket propulsion systems which are optimally adapted to their foreseen mission. Different missions and applications can include sounding rockets, suborbital space flight, micro launchers,[3)] boosters, deorbiting systems,[4)] apogee motors,[5)] or even lunar or Martian landers and sample return vehicles.[6,7)] In order to analyze complete missions with hybrid rocket propulsion with flexible mission objectives both the trajectory with its different phases and impulsive maneuvers and the hybrid propulsion system with all its parameters like thrust level, chamber pressure, propellant combination et cetera must be simulated and optimized. Astos Solutions GmbH in Germany offers the very versatile software "AeroSpace Trajectory Optimization Software" (ASTOS). ASTOS gives the possibility to model any mission in space transportation from launcher ascent via in-orbit operations through to landings on other celestial bodies. Propulsion systems are modeled with tables and performance parameters. However a detailed simulation of a hybrid propulsion system is not yet included. EcosimPro with its library European Space Propulsion System Simulation (ESPSS) is developed by Empresarios Agrupados in Spain at behalf of the European Space Agency ESA. EcosimPro with ESPSS is a system simulation tool for space propulsion systems with high flexibility and a great level of detail. It is possible to simulate different liquid rocket engines with or without turbopumps, tanks, pipes, valves, cooling channels and so on. Since the newest version of ESPSS hybrid rocket engines are also part of the ESPSS library. Therefore the idea was born to implement an interface between both tools to combine the possibilities of trajectory optimization and propulsion system simulation. In cooperation with ESA ESTEC this interface is created at the DLR Lampoldshausen. For hybrid rockets it is especially useful to have a combined trajectory simulation and optimization, because hybrid rocket engines commonly have time dependencies in their performance. The chamber geometry changes as the fuel regresses and therefore the mixture ratio, thrust and

chamber pressure change over burning time. Often the engine parameters can be optimized to have the perfect working point for the engine respecting efficiency and thrust, but sometimes these optimum working points are not the best choice for an actual mission. Other aspects like throttle-ability or engine and tank size and weight are also of high impact. Therefore a combined optimization of both propulsion system and trajectory offers advantages to quickly adapt the hybrid propulsion system to any mission. As an example of optimization both a hybrid micro launcher and a lunar lander module are designed and optimized with the toolset. Different propellants can be compared. Classical hybrid fuels like hydroxyl-terminated polybutadiene (HTPB) can be compared to advanced fuels like paraffin-based fuels, which offer much faster regression rates and can improve the engine's performance greatly. Liquid oxygen offers the highest specific impulse as an oxidizer in a hybrid rocket engine, however, from a mission analysis point of view, hydrogen peroxide can be an adequate choice as well, as it isn't cryogenic and its high density decreases the tank size and mass.

2. Software Tools

2.1. Trajectory Optimization with ASTOS

ASTOS offers the possibility to design, simulate, optimize and analyze any kind of trajectory to and in space with 3-DOF or 6-DOF equation of motions. ASTOS is highly flexible and very detailed. Possible trajectories are aerodynamically stable sounding rockets, heavy launch vehicles, orbit maneuvers of spacecraft, rendez-vous missions or planetary landing missions. The vehicle or spacecraft can be customized with a library of components including stages, tanks, payload etc. Usually aerodynamics as well as the propulsion system's performance is described with constants or tables. For the propulsion system the respective parameters are propellant mass flow and vacuum impulse. The user can set different constraints for the optimizer to define the final trajectory. The optimizer can optimize hundreds or thousands of parameters using multiple shooting or collocation methods within the CAMTOS optimizer.[8] Depending on the trajectory and its characteristics, the user can choose the better fitting method. Multiple shooting is advantageous for trajectory phases with high derivatives like high accelerations. Collocation is faster in computational time in long phases like coast arcs. Optimization parameters can be propulsion parameters like thrust and thrust throttling, attitude control, propellant and payload masses. With so called cost functions the user can set certain parameters to be either minimized, for example integral heat load during reentry or total gross lift off mass of a launcher, or maximized like a launcher's payload.

2.2. Analytical hybrid propulsion component

In order to improve the simulation detail of propulsion systems, instead of a simple input like a mass flow and vacuum impulse table over time, ASTOS includes a user propulsion model interface in C programming language. This interface is used to include a more detailed simulation of a hybrid propulsion system. The first part of this user propulsion model is an analytical model of a hybrid combustor to calculate the fuel mass flow and the vacuum impulse for a given oxidizer mass flow and combustion chamber geometries. The critical part of this model is the regression rate simulation. A simplified approach is to calculate the regression rate with the oxidizer mass flux density as

$$\dot{r}_f = aG_{ox}^n. \tag{1}$$

This approach is used in many experimental works e.g. by Karabeyoglu.[9] It can be applied both for classical and liquefying hybrid rocket fuels. However, it is not precise for hybrid engines where the solid fuel's regression rate is not uniform over the length of the fuel grain as well as for hybrid combustors where lateral combustion plays a role. But for a first approximation of the performance of an engine it is satisfying. The regression parameters a and n are user inputs. Further user inputs are next to the combustion chamber geometry the combustion efficiency η_{c^*} and thrust efficiency η_{c_F}. The benefit of this model is, that the computational time is very low, so that it can actually be used for optimization. Optimizable parameters can include the combustion chamber and fuel grain geometry, the nominal oxidizer mass flow and the throttle. In this way, ASTOS can optimize the trajectory and the hybrid rocket engine at the same time. Also an estimation of the combustion chamber mass is implemented. Therefore, the optimization can also consider the structural mass of the spacecraft and propulsion system.

2.3. ESPSS model for hybrid propulsion

The software platform EcosimPro offers a simulation platform for modeling 0D or 1D systems of differential-algebraic equations. The library ESPSS includes many components for modeling complex propulsion systems: Tanks, combustion chambers, pipes, cooling systems, fluid control, turbopumps, etc. The goal of including an ESPSS model for the hybrid propulsion system in ASTOS is, that with this a much more detailed simulation can be done. The ESPSS model can be as simple as a valve, pipe and combustion chamber, but it can also include tanks and pressurization systems. For an even more sophisticated spacecraft simulation it could include even a RCS thruster system. Regarding the hybrid combustor there is a large advantage compared to the analytical formulation: the combustion chamber can be modelled in high detail. The chamber itself is discretized in one dimension. This means, pre- and post-combustion chambers can be represented as well as segmented fuels with different diameters. Additionally lateral regression of the fuel can be simulated. The simulation of the combustion process itself is also much more detailed: the vaporization of a liquid oxidizer as well as the vaporization of the solid fuel is modelled with all necessary heat flows, thermal losses to the combustion chamber wall are regarded, and chemical processes taking place along the chamber's x-axis are considered instead of taking place instantaneously. The largest difficulty in simulating hybrid rocket engines is to properly model the regression rate. The hybrid combustor component in ESPSS is provided with three regression rate models:

1. Regression rate based on coefficients a and n with the local mass flux G. Here the discretization in 1D of the fuel is of advantage. The local mass flux G at every node can be used to calculate the regression rate with

$$\dot{r}_f = aG^n. \tag{2}$$

But to use this equation the parameters a and n need to be known. In experimental tests it is difficult to get the

parameters for the local mass flux. This is why often the coefficients are only known with averaged values over the experimental data for the oxidizer mass flux G_{ox}.

2. Therefore, the second option is to use the same equation but with the oxidizer mass flux G_{ox}. Those two empirical models for the regression rate also neglect the influence of the axial position along the fuel grain.
3. The third regression model supplied by ESPSS is a vaporization model, which uses the energy balance at the solid fuel's surface to calculate vaporization and therefore a regression rate. However, this model is very simplistic and does not take into account phenomena that have been described already by Marxman in the 1960's.[10] Therefore this model should not be used in its current state. The model highly overestimates the regression rate.

Three further models are implemented in addition to those included in the ESPSS standard hybrid rocket combustor component.

1. The before mentioned regression rate model by Marxman was implemented into the ESPSS component. The formulation for the regression rate is:

$$\dot{r}_f = 0.036 \frac{G^{0.8}}{\rho_s} \left(\frac{x}{\mu_m} \right)^{-0.2} \left(\frac{u_e}{u_c} \frac{\Delta h}{h_{vap}} \right)^{0.23} \tag{3}$$

In this model, no experimentally determined coefficients are necessary. Instead, fuel properties need to be given as input: The fuel density ρ_s, the combustion gas viscosity μ_m as well as the ratio of the velocity of the gas in the core stream (equal to boundary layer edgevelocity) and the flame $\frac{u_e}{u_c}$ and the ratio of total enthalpy difference between flame and fuel to the effective heat of vaporization $\frac{\Delta h}{h_v}$. Marxman's law was derived for a flat fuel slab. In a cylindrical combustion chamber the effect of the position x along the fuel grain is smaller than on a single sided plate, because the distance between the flame and the fuel grain has a maximum and cannot grow any further when a full pipe flow has been established. Marxman's law therefore predicts too small regression rates for large x-positions in cylindrical combustion chambers.

2. In 2006 Zilliac and Karabeyoglu published a new regression rate law for classical hybrid fuels based on Marxman's theory.[11] This regression rate law is adapted to the behavior of the flow inside a cylindrical fuel port. This law has also been implemented into ESPSS.
3. Finally the regression rate model for liquefying fuels by Karabeyoglu et al[12] has been implemented to simulate also the regression of liquefying fuels like paraffin-based fuels. This model considers the melt layer, that liquefying fuels form on their surface. The melt layer thickness is calculated. When the turbulence in the boundary layer is high enough, wavelets are formed on the surface of the liquid. Droplets are entrained on top of these wavelets into the core flow. These droplets are not vaporizing in the boundary layer but in the core flow. Therefore they increase the fuel mass transfer without increasing the necessary enthalpy flow from the flame to the fuel surface. This increases the regression rate by a factor up to five compared to classical hybrid fuels.

2.4. Regression law simulation results

Figure 1 shows the schematic of a simple test model, which was used to compare the results of the different regression rate models. It is set up with an inflow condition, a working fluid definition, a mass flow controller, the modified combustion chamber model and two isolations for the injector dome and the combustion chamber wall. The simulations were done with a mass flow of $\dot{m}_{ox} = 3.5\,\mathrm{kg/s}$. The fuel grain was defined as 1.8 m long, divided into six uniformly long nodes with an inner diameter of 80 mm and an outer diameter 120 mm. The nozzle throat diameter is 60 mm, resulting in a chamber pressure of about 28 bar. In Figure 2 the regression rate results are illustrated us-

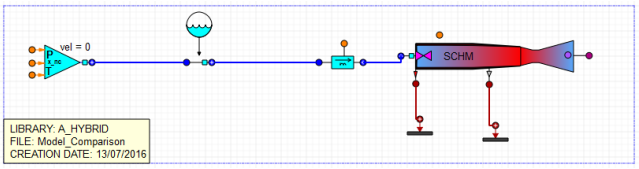

Fig. 1. Simple ESPSS model to compare the regression rate laws

ing the model by Marxman. It is visible that the regression rate for the nodes to the rear is quickly reduced. This model is underestimating the heat transfer between flame and fuel towards the fuel grain's end, as it is overestimating the distance between flame and fuel, as well as the so called blocking effect. This relates to the fuel vapor mass flow ejected from the fuel's surface actually blocking the heat transfer from the flame to the fuel. In contrast to the results obtained with Marxman's model, Fig-

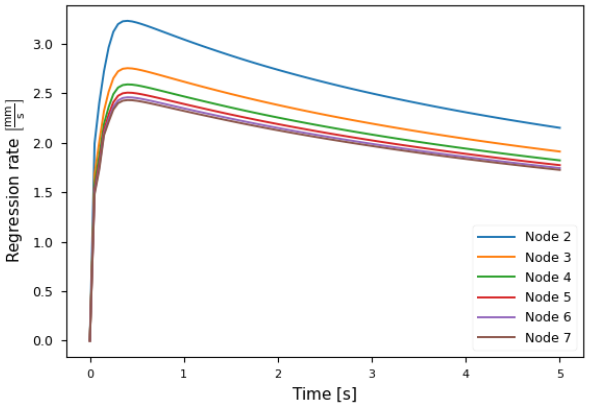

Fig. 2. Example regression rate simulation with Marxman's theory law

ure 3 displays the results with the regression rate model by Zilliac. Here the regression rate at the first node is much smaller compared to Marxman's model, however, the regression rate downstream along the fuel grain is increasing. This is in better agreement to experiences gained in experiments. However, for very long fuel grains, the regression rate should reach a maximum at some point. This is also correctly represented with Zilliac's model. For very long fuel grains, the regression rate is not increasing at the rear end anymore. Figure 4 compares all the different models at the fourth node. "stdHybrid_Gox" is the model based on the regression rate coefficients and the oxidzer mass flux G_{ox}. "stdHybrid_G" is based on the local mass flux G instead. The coefficients for both of these simulations have been taken from literature with $a = 0.0903\,\mathrm{mm/s}$ and $n = 0.527$.[11] "vapModelimproved" is a simple model based

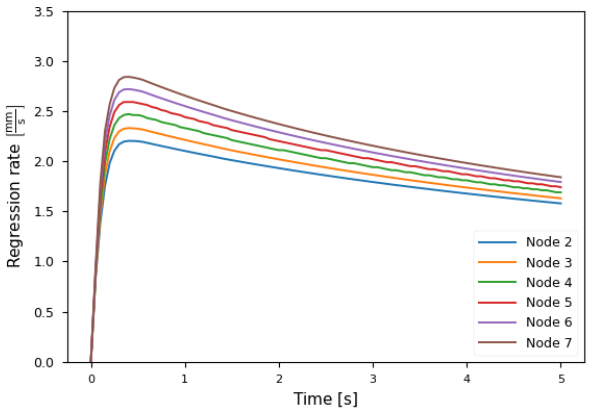

Fig. 3. Example regression rate simulation with Zilliac's theory law

on the standard vaporization model of ESPSS, which takes the enthalpy balance at the fuel's surface to calculate the regression rate. However, it is not considering turbulence and flow effects. This is why it underestimates the regression rate, while all other models at least for the node 4 in the middle of the fuel grain are at similar regression rate values. All regression rate models are

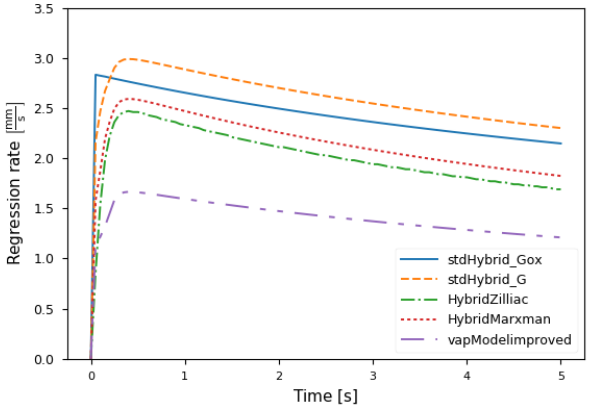

Fig. 4. Comparison of regression rates with different laws at node 4

very sensitive to the input parameters. For the regression rate coefficients a and n many experiments need to be evaluated in order to cover all propellant combinations, chamber geometries and mass flux ranges. The input values of the other regression rate models are listed in Table 1. For the future, some of these input parameters like flame zone temperature T_c or flame zone mixture ratio $^O/_{F_c}$ could be modelled as well to reduce number of input parameters. To compare simulation results with experimental data the regression rate models based on coefficients a and n are always the best suited. Also to predict performances of a similar fuel grain geometry after up- or downscaling these models promise the best results, even if scale effects need to be considered. Scaling up usually decreases the regression rate a bit. If a new fuel is investigated, where no experimental data is available, the regression rate laws by Marxman and Zilliac can give a first estimation of the fuel's regression rate for classical fuels. For liquefying fuels Karabeyoglu's model can be used. Thereby it is easier to pre-design a rocket engine for a new fuel for the first experiments. However, both laws are not able to replace experimental investigations of a propellant combination's fuel regression rate. For the simulation and optimization of trajectories with ASTOS the regression rate law based on coefficients is used in the analytical model (see section **3.1.**). However, the other regression laws can be used to get predicition of the effect, which the regression rate uncertainties in a new hybrid rocket engine can have on the performance and the trajectory. Coupling between ASTOS and ESPSS simulation is done with correction factors. First the trajectory is simulated and optimized with the analytical model. Then with the optimized parameters and control an ESPSS simulation is done to verify the performance results. In case the oxidizer and fuel mass flow or specific impulse deviates between the results gained with the analytical tool and the ESPSS simulation, correction factors for those three parameters are implemented which will scale the analytical results to match the ESPSS simulation. The analytical tool is simplified, therefore almost always a deviation in the results can be expected. Time dependent gradients and 1D effects can only be simulated in ESPSS. After applying correction factors to the analytical model a new optimization process can be started. This is an iterative process and allows to consider also effects, that are covered by ESPSS but not by the analytical tool, for example lateral regression.

Table 1. Regression rate model inputs

Name	Symbol	Model
Specific heat of flame gas	$c_{p,c}$	Marxman, Zilliac
Specific heat of fuel vapor	$c_{p,f,vap}$	Marxman, Zilliac
Flame mixture ratio	$^O/_{F_c}$	Marxman, Zilliac
Flame temperature	T_c	Marxman, Zilliac
Latent heat of vaporization	L_{vap}	Marxman, Zilliac
Mean viscosity	μ_m	Marxman, Zilliac
Oxidizer concentration	K_{ox}	Marxman, Zilliac
Vaporization temp. of fuel	T_{vap}	Marxman, Zilliac
Activation energy	E_a	Zilliac
Heat conduct. of fuel vapor	k_f	Zilliac

3. Optimization of test cases

3.1. Optimization process

The optimization of the following two test cases, a hybrid micro launcher and a lunar lander, was done in these steps:

1. Create an initial guess: For the initial guess with ASTOS all mission phases, vehicle parameters (e.g. propellant masses or engine geometries) and controls (throttle, attitude) need to be set. The initial guess for the trajectory should usually be already very close to the optimum result, in order to increase convergence of the gradient based CAMTOS optimization. During the initial guess, for all optimizable parameters and controls boundaries need to be set.
2. Optimize trajectory: The first optimization is done to actually reach a trajectory which meets the final constraints and requirements, e.g. circular orbit for a launch vehicle and soft landing on the moon for the lander.
3. Optimize the vehicles for either minimum initial mass or maximum payload.
4. Repeat the last step and check if any boundaries are reached and need to be modified.

5. When the optimization is at an optimum and all constraints and goals are met, a simulation with the ESPSS interface was done to get the values of the correction factors
6. Repeat the optimization process with the correction factors included for the analytical hybrid rocket engine model. This can be done a few times, until the simulation with ESPSS does not change the correction factors anymore.

3.2. Hybrid micro launcher

3.2.1. Model set-up

One field of application for hybrid rocket engines are small-lift launch vehicles, especially with small payloads for example up to 500 kg. The interest in this kind of launchers has grown in the last years, as miniaturization of satellites has progressed, and even small satellites can do many experiments and observations. Also the plans for satellite constellations consisting of hundreds or thousands small satellites in the near future have driven the development of small, flexible launch vehicles. According to the definition for micro satellites, which have a mass of 10 to 100 kg, a micro launcher based on hybrid rocket engines, with a payload of 25 kg to a 250 km circular polar orbit was defined, simulated and optimized. As hybrid rocket engines get problematic with long burning durations, because their diameter grows steadily, a three-stage concept was initiated. Table 2 shows the trajectory phases of the optimized mission. The first stage burns during the first four phases, after which the stage separation is conducted. First simulations showed, that after the first stage the rocket's apogee is already close to the final orbit altitude. This is why a long ascent coast is inserted. After the rocket ascents to high altitudes, the second stage is ignited in order to raise the perigee. After another coast the third stage is ignited to reach the final circular orbit. The arrow symbol "→" indicates the change from the initial guess to the optimized parameter value. In order to produce the desired optimal result, several boundary constraints need to be set in the ASTOS model. Table 3 presents a list of the active constraints in this model. None of the mentioned boundary constraints are unique to a hybrid rocket. These constraints are rather the minimum set of constraints necessary to optimize a three stage launch vehicle to a circular orbit. Table 4 shows the inital and optimized

Table 2. Trajectory phases

Name	Description	Duration		
1. Lift-Off	Vertical take-off	0.2 s	→	0.1 s
2. Pitch Over	Constant pitch rate	11.8 s	→	4.1 s
3. Pitch Constant	Transition to gravity turn	6 s	→	3.3 s
4. Gravity Turn	Angle of attack is zero	47 s	→	42.5 s
5. Ascent	Ascent with stage separation	130 s	→	100.2 s
6. Stage 2 burn	Orbit raising	35 s	→	43.8 s
7. Coast	Coast to apogee	20 s	→	34.6 s
8. Stage 3 burn	Final orbit raising	65 s	→	98.8 s

mass parameters for the micro launcher concept. The structural masses are rough estimations and were not changed during the optimization progress. The study's main goal was to prove that

Table 3. Optimization constraints for a micro launch vehicle

Type	Constraint	Bounds	Phase
Init	Initial position	0 m, 68 °N, 21 °E	1
Init	Init. radial velocity	0 m/s	1
Init	Init. north vel.	0 m/s	1
Init	Init. relative east vel.	0 m/s	1
Path	Pitch rate	±2.5 °/s	2,6,8
Path	Yaw rate	±2.5 °/s	2,3,6,8
Path	Gravity turn cond.	±0.3 °	4
Final	Max. orbital inclin.	95 °	4,6,8
Path	Max. acceleration	130 m/s²	4,6,8
Final	Apogee	250 ± 5 km	8
Final	Altitude	250 ± 5 km	8
Final	Perigee	250 ± 5 km	8
Final	Orbit inclination	94.5 ± 0.5 °	8

the modelling of hybrid rocket engines is correct and that the optimization process is working. The claim was not to optimize a real micro launcher concept for practical realisation. However this work can be the foundation for further studies in that field. Especially the aerodynamics and the mass estimation for the hybrid rocket engine need to be improved. In Table 5 the

Table 4. Initial and optimized micro launcher masses

St.	Component	Initial mass	Optimized
1	Propellant	13400 kg	→ 8268.3 kg
	Tank structure	7.53 % of oxidizer mass	
	Engine structure	620 kg	→ 400 kg
	Additional Structures	310 kg	
	Total Stage Mass	15232 kg	→ 9548.9 kg
2	Propellant	1525 kg	→ 1538.2 kg
	Tank structure	8.77 % of oxidizer mass	
	Engine structure	130 kg	→ 114 kg
	Additional Structures	110 kg	
	Total Stage Mass	1883.2 kg	→ 1881.05 kg
3	Propellant	132 kg	→ 179.1 kg
	Tank structure	9.8 % of oxidizer mass	
	Engine structure	13.5 kg	→ 15.5 kg
	Additional Structures	35 kg	
	Total Stage Mass	216.9 kg	→ 270.1 kg
	Payload	25 kg	
	Fairing	10 kg	
	Total Lift Off Mass	**17332 kg**	**→ 11700 kg**
	Total Prop Mass	**15057 kg**	**→ 9985.6 kg**

initial and optimized engine parameters are listed. The propulsion system is designed to use paraffin-based fuel and H_2O_2 as an oxidizer. The first stage uses seven parallel rocket engines fed from one oxidizer tank, while the second stage uses four parallel engines. The upper stage uses a single engine. The optimizer can also change the throttle of all three stages. The nominal thrust, nominal mean mixture ratio and the burn time per engine are listed in the table. Table 6 shows the optimizable parameters, that define the hybrid rocket engines of the three stages.

Table 5. Initial and optimized micro launcher propulsion system

Stage	Engine thrust	$\overline{O/F}$	Burn time
1	73 kN → 61 kN	7.6 → 9.0	65 s → 50 s
2	30 kN → 28 kN	7.6 → 7.4	35 s → 43.8 s
3	5 kN → 6 kN	7.6 → 7.6	65 s → 98.8 s

Table 6. Engine parameters

St.	Component	Initial value	Optimized
1	Fuel length	1.6 m	→ 1.25 m
	Fuel diameter	480 mm	→ 415 mm
	Throat diameter	139 mm	→ 135 mm
	Expansion ratio	6	→ 4
2	Fuel length	965 mm	→ 915 m
	Fuel diameter	300 mm	→ 285 mm
	Throat diameter	92 mm	→ 85 mm
	Expansion ratio	50	→ 51
3	Fuel length	412 mm	→ 412 m
	Fuel diameter	270 mm	→ 274 mm
	Throat diameter	38 mm	→ 33 mm
	Expansion ratio	60	→ 170

3.2.2. Optimization results

The initial guess of the trajectory did not reach a circular orbit. The initial trajectory was a suborbital trajectory with an apogee at 420 km and a perigee at -490 km. The optimization goal was therefore to reach the defined final orbit and at the same time reduce the launcher mass. Some of the optimization results are already shown in the tables 2, 4, 5 and 6. To reach the final orbit, the burn phases of the second and third stages were prolonged, while the first stage's burn duration was reduced by 15 seconds. The maximal thrust level of the first and second stage was reduced, due to the lowered total mass. The total launcher mass was reduced by 5632 kg (32.5 %). Most of this was saved in propellant mass, where 5071.4 kg (33.7 %) was saved. This was reached by optimizing the mixture ratio O/F and optimizing the expansion ratio as well as the chamber pressure. The expansion ratios however were limited by the stage diameters. There is one limitation in the current model: The optimizer increased the chamber pressure by reducing the throat diameter in all engines, see Table 6. This increases the vacuum impulse and decreases engine mass, because the nozzle is getting smaller. However, this would require a higher tank pressure or a pump, which is currently not taken into account for the optimization's mass balance. This is a necessary step to improve the model. However, the first optimization results still are very promising. In total, the first stage was reduced most in size, while the propellant of stage two and three was increased. This is expected, as the first stage has the lowest specific impulse due to the limited expansion ratio. Additionally a larger first stage increases aerodynamic and gravitational losses. The optimization of the model was successfull and it is a proof that the combined optimization of the trajectory and the engine with the analytical model works as expected. The thrust of the first stage is throttled down 20 seconds after lift-off. Figure 5 displays exemplarily the optimized acceleration, thrust and oxidizer mass flow of the second stage during its burn. The mass flow is for a single engine. The oxidizer mass flow, which is the controlled input of the engine model, is throttled down after optimization during the beginning and in the end of the phase. While for the throttling down at the end the cause is quite obvious, the reason for the small downthrottling at the beginning is not clear. It can have many reasons. The optimization is a multidimensional problem, and it is not always easy to understand the mechanisms that prefer one solution over another. This is also one reason for using numerical optimization, because this kind of problem cannot be solved analytically. A possible explanation for the reduced thrust in the first stage and in the beginning of the second stage's burn is that at this part of the trajectory gravitational losses are higher. At the end of the second burn the vehicle's acceleration increases as the mass is reduced every second. Therefore the acceleration reaches the limit of 130 m/s^2 and the four engines of the second stage are throttled down. The acceleration at the phase's end is approximately 130 m/s^2. The limit of 130 m/s^2 was chosen to demonstrate that the path constraints work. The limit is still a bit too high for real applications. For future optimizations a applicable limit according to the payload's requirements will be used. The regression rates and mixture ratios of the three stages' engines are shown in Figure 6. The regression rate of stage 1 and 2 are in a similar range, only the regression rate of the third stage is lower. This is due to the lower mass flux G in this engine, which is also necessary to sustain longer burn times. The mixture ratios of stage one and two show, that the throttling has a major effect on the mixture ratio. The mixture ratio drops by about 10 %. For the propellant combination H_2O_2 and paraffin-based fuel the gradients of the function of specific impulse over mixture ratio are quite small. Therefore this oxidizer could be especially useful for throttling engines. The loss in specific impulse in this case is only 1 % from 2900 m/s to 2870 m/s. Figure 7 displays some trajectory parameters over time to visualize the optimized ascent to the low Earth orbit. Figure 8 illustrates the layout of the micro launcher. It also shows the proportions of stages, engines and tanks. The base diameter is 1.5 m without fins and the length is 12.5 m. Table 7 lists the applied correction factors determined with the ESPSS interface.

Table 7. Optimization correction factors

St.	Oxidizer mass flow	Fuel mass flow	Specific impulse
1	99.30 %	98.97 %	103.16 %
2	99.91 %	99.36 %	100.83 %
3	100.31 %	99.670 %	108.8 %

3.3. Simulation and optimization of a lunar lander

A hybrid propulsion lunar lander with a sample return rocket was introduced in a previous work.[6] The mission is designed to be launched with an Ariane 5 or comparable launcher to a direct Moon orbit transfer. The initial Moon orbit of the vehicle is a hyperbolic fly by with a low perilun of about 100 km. At the perilun the first of two hybrid rocket kick stages is ignited to lower the perilun to about 10 km altitude. Then the emtpy stage is ejected and after a coast the second kick stage is ignited at the new perilun of 10 km. The second stage is reducing the horizontal and vertical velocity close to zero, then it is ejected and the lunar lander starts its final vertical descent. The mass of the lander and the kick stages in total is 8300 kg with Paraffin-based fuel and 95% hydrogen peroxide as oxidizer. Previously

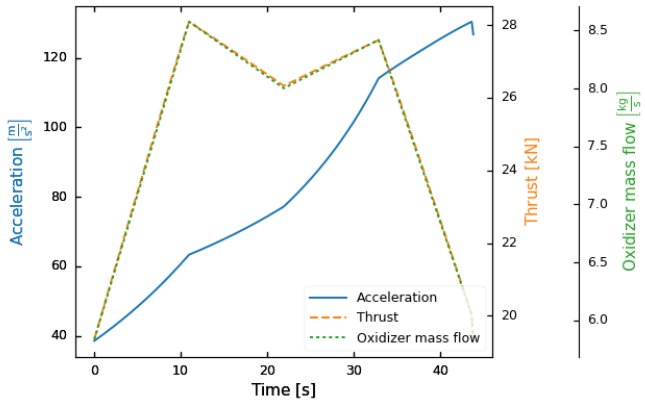

Fig. 5. Acceleration, thrust and oxidizer mass flow during second stage burn

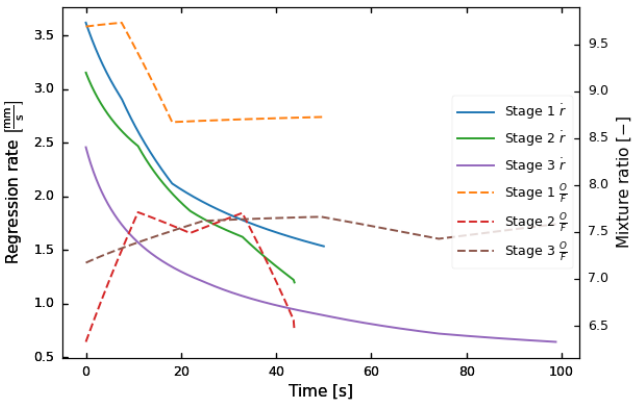

Fig. 6. Regression rates and mixture ratios of the three stages

the simulation and optimization of the lander and its trajectory was done using only rough estimations of the propulsion systems' performance. A constant performance was assumed. Now the simulation and optimization has been renewed with the new ASTOS and ESPSS interface for hybrid propulsion systems. One change that has been done to the original model was the engine set-up. The four parallel engines on each kick stage were replaced by one larger hybrid rocket engine. This change was possible, since new regression rate results in experiments

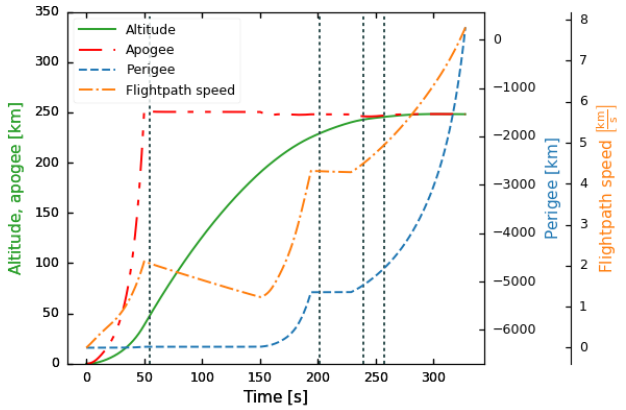

Fig. 7. Altitude, apogee, perigee and flightpath speed

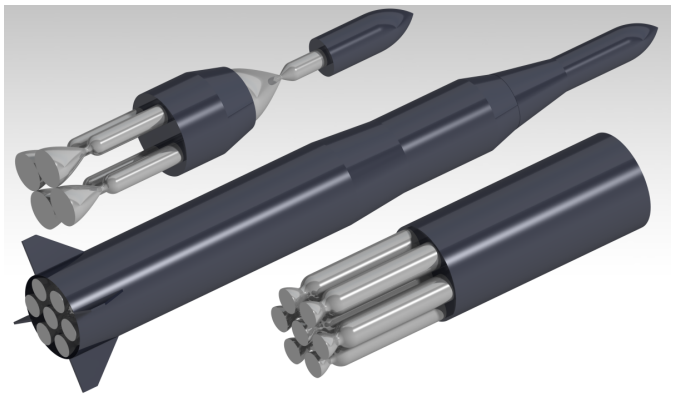

Fig. 8. A preliminary design of a three stage micro launcher

showed, that it can be feasible to have one large long burning hybrid rocket engine. The optimum in terms of structural mass to fuel ratio has to be found in the future. Table 8 displays the lunar lander mass before and after optimization of the trajectory. In total 200 kg of H_2O_2 are included for RCS thrusters. The payload includes the return rocket as well as power supply and instrumenation of the lander. It can be seen that the payload and masses were not improved a lot by the optimizer. The reason for this is, that the inputs were already taken from the optimized trajectory of the previous work. However the trajectory itself was optimized, as well as the rocket engine's geometries which is listed in Table 9. Figure 9 shows the altitude and periapsis altitude of the lander. Both initial guess and optimized curves are printed. The initial guess is not very close to a realistic descent on the Moon's surface. The descent rate at the end is increasing, which can be also seen in Figure 10. Even though the initial guess was not very good, the optimization with Astos found an optimal trajectory which would meet the conditions of a soft touch down. Figure 11 shows a detailed view of the final landing. It features the end of the second kick stage's burn until 3300 s, a short coast of 25 s and a nearly vertical descent until touch down with a flight path speed of about 1.5 m/s. A first impression of the possible landing module with a return rocket is pictured in Figure 12. The combustion chambers and nozzles as well as the H_2O_2 tanks are in true scale both for the landing craft and the return rocket. The diameter of the truss is about 2.5 m and the height is about 3.1 m.

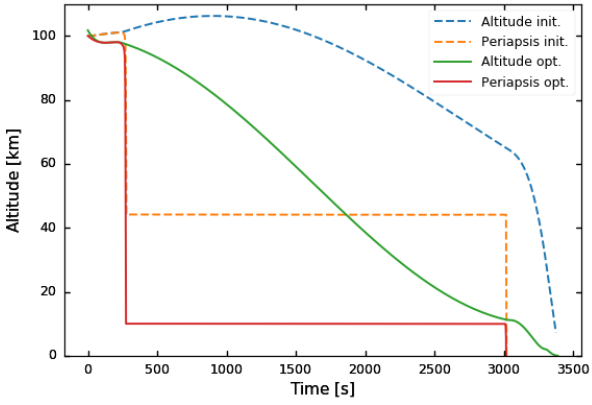

Fig. 9. Altitude and periapsis of the lander before and after optimization

Table 8. Initial and optimized lunar lander masses

St.	Component	Initial mass	Optimized
1	Propellant	2300 kg	→ 2302 kg
	Tank structure	4 % of oxidizer mass	
	Engine structure	115 kg	→ 115 kg
	Additional Structures	355 kg	
	Total Stage Mass	2852 kg	→ 2851 kg
2	Propellant	2550 kg	→ 2497 kg
	Tank structure	4 % of oxidizer mass	
	Engine structure	115 kg	→ 115 kg
	Additional Structures	380 kg	
	Total Stage Mass	3135 kg	→ 3079 kg
3	Propellant	290 kg	→ 171 kg
	Tank structure	9.8 % of oxidizer mass	
	Engine structure	10 kg	→ 10 kg
	Additional Structures	920 kg	
	Total Stage Mass	1230 kg	→ 1167 kg
	Payload	1217 kg	→ 1200 kg

Table 9. Lunar lander engine parameters

St.	Component	Initial value	Optimized
1	Fuel length	850 mm	→ 830 m
	Fuel diameter	720 mm	→ 720 mm
	Throat diameter	104 mm	→ 104 mm
	Expansion ratio	180	→ 182.5
2	Fuel length	850 mm	→ 849 m
	Fuel diameter	720 mm	→ 740 mm
	Throat diameter	104 mm	→ 100.6 mm
	Expansion ratio	180	→ 190
3	Fuel length	155 mm	→ 160 m
	Fuel diameter	140 mm	→ 144.5 mm
	Throat diameter	18 mm	→ 15.1 mm
	Expansion ratio	190	→ 200

4. Conclusion

Hybrid rocket engines have emerged in the last year to higher technology levels. For several applications hybrid rocket engines can compete with liquid systems or surpass solid rocket motors. One problem with hybrid rocket motors is the proper predicition of regression rate. EcosimPro with ESPSS is a powerful tool for rocket cycle analysis and rocket engine simulation. With the addition of new state of the art regression rate laws for both classical and liquefying solid fuels the predictions of hybrid rocket engines' performance with ESPSS can be improved, especially if only few or no experimental data are available for the respective propellant combination. The combination of hybrid rocket engine simulation with trajectory simulation and optimization is successfully realized with an interface between ASTOS and ESPSS. An analytical model for the performance of the hybrid rocket engines is used for creating initial guesses and optimization of the trajectory. A comparative simulation with an ESPSS interface in ASTOS can be done to consider more complex processes that are included in the ESPSS model, like lateral combustion, heat transfer to the engine wall and transient processes. A correction factor for mass flows and specific impulse is calculated and can be applied to optimize the trajectory again. With this tool a complete optimization and analysis of a vehicle and its trajectory can be done. For the future this tool can accelerate the design of any hybrid rocket engine powered vehicle like small launch vehicles, sounding rockets, planetary landers or in orbit servicing spacecrafts.

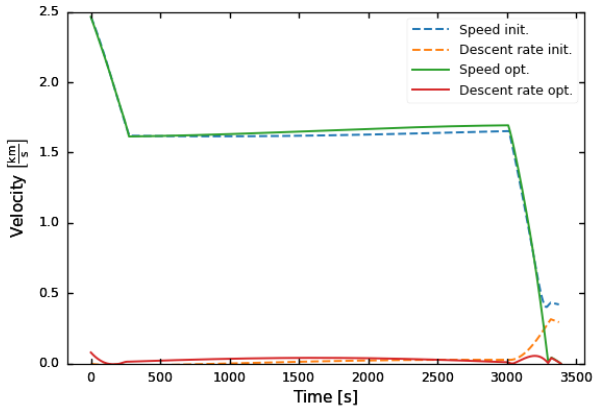

Fig. 10. Speed and descent rate of the lander before and after optimization

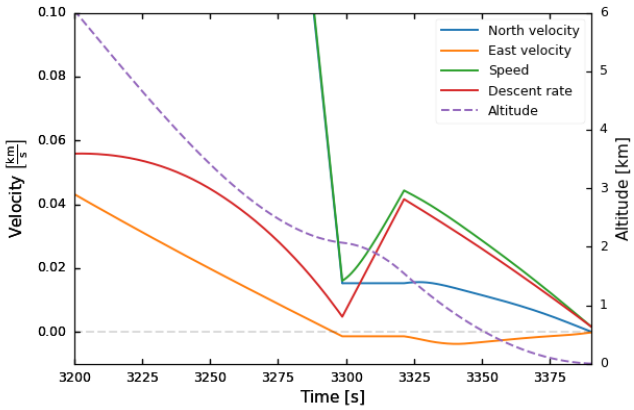

Fig. 11. Velocities and altitude of the lander in the final landing sequence

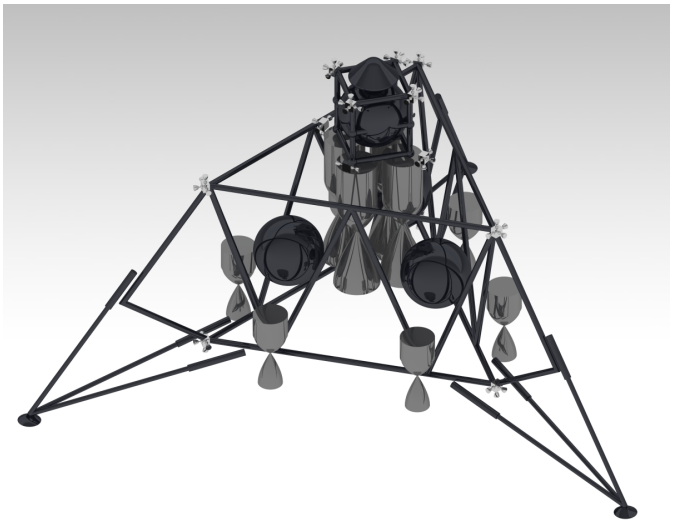

Fig. 12. Preliminary illustration of the lunar lander module with a return rocket

References

1) Kobald, M., Schmierer, C., Ciezki, H., Schlechtriem, S., Toson, E. and De Luca, L. T.: *Viscosity and Regression Rate of Liquefying Hybrid Rocket Fuels*, Journal of Propulsion and Power, Vol. accessed March 16, 2017
2) Kobald, M., Schmierer, C., Fischer, U., Tomilin, K.: *A Record Flight of the Hybrid Sounding Rocket HEROS 3*, 31st ISTS, 2017
3) Verberne, O., Boiron, A., Faenza, M., Haemmerli, B.: *Development of the North Star Sounding Rocket: Getting ready for the first demonstration Launch*,51st AIAA Joint Propulsion Conference, 2015
4) Faenza, M., Verberne, O., Tonetti, S., Cornara, S., Langener, T.: *Hybrid Propulsion Solutions for Space Debris Remediation Applications*, Industrial Days ESA ESTEC, 2016
5) Odic, K., Denis, G., Ducerf, F., Martin, F., Lestrade, J., Verberne, O., Ryan, J., Christ, P., de Crombrugghe, G.: *HYPROGEO Hybrid Propulsion: Project Objectives & Coordination*, Space Propulsion, Rome, 2016
6) Schmierer, C., Tomilin, K., Kobald, M., Steelant, J. and Schlechtriem, S.: *Analysis and Preliminary Design of a Hybrid Propulsion Lunar Lander*, Space Propulsion, Rome, 2016
7) Chandler-Karp, A., Nakazono, B., Benito, J., Shotwell, R., Vaughan, D., Story, G.: *A Hybrid Mars Ascent Vehicle Concept for Low Temperature Storage and Operation*, 52nd AIAA Joint Propulsion Conference, 2016
8) Gath, P.: *CAMTOS - A Software Suite Combining Direct and Indirect Trajectory Optimization Methods*, University of Stuttgart, 2002
9) Karabeyoglu, M. A., Zilliac, G., Cantwell, B. J., DeZilwa, S. and Castellucci, P.: *Scale-up tests of high regression rate paraffin-based hybrid rocket fuels*, Journal of Propulsion and Power, American Institute of Aeronautics and Astronautics, 2004, Vol 20, pp.1037-1045
10) Marxman, G. et al: *Fundamentals of Hybrid Boundary Combustion*, Progress in Astronautics and Aeronautics, 1964
11) Zilliac, G. and Karabeyoglu, M. A.: *Hybrid Rocket Fuel Regression Rate Data and Modeling*, 42nd AIAA/ASME/SAE/ASEE Joint Propulsion Conference and Exhibit, 2006
12) Karabeyoglu, M. A., Altman, D. and Cantwell, B. J.: *Combustion of liquefying hybrid propellants: Part 1, general theory*, Journal of Propulsion and Power, American Institute of Aeronautics and Astronautics, 2002, 18, 610-620